Non-linear modal interactions in free-edge thin spherical shells: Measurements of a 1:1:2 internal resonance

Olivier Thomas, Cyril Touzé, Éric Luminais

Non-linear modal interactions in free-edge thin spherical shells: measurements of a 1:1:2 internal resonance

Olivier Thomas[a,*], Éric Luminais, Cyril Touzé[b]

[a]Structural Mechanics and Coupled Systems Laboratory, CNAM, 2 rue Conté, 75003 Paris, France
[b]ENSTA-UME, Chemin de la Hunière, 91761 Palaiseau Cedex, France

This study is devoted to the experimental validation of a theoretical model of large amplitude vibrations of thin spherical shells described in Thomas et al.[1]. A specific mode coupling due to a 1:1:2 internal resonance between an axisymmetric mode and two companion asymmetric modes is especially addressed. The structure is forced with a sinusoidal signal of frequency close to the natural frequency of the axisymmetric mode. The experimental setup, which allows precise measurements of the vibration amplitudes of the three involved modes, is presented. Experimental resonance curves showing the amplitude of the modes as functions of the driving frequency are compared to the theoretical ones. A good qualitative agreement is obtained with the predictions given in the model. The quantitative discrepancies are discussed and an improvement of the model is proposed.

Keywords: Shallow spherical shells; Geometrical non-linearities; Internal resonances; Non-linear vibrations; experiments

1. Introduction

In an earlier paper [1], a theoretical model of a spherical shell subjected to large amplitude asymmetric non-linear vibrations was derived, using the analog for thin shallow shells of von Kármán equations for plates. This paper presents a series of measurements in order to validate the theoretical developments of Thomas et al. [1], in the special case of a 1:1:2 internal resonance, observed with a harmonic forced excitation.

Asymmetric non-linear vibrations of spherical shells have received little attention, as opposed to the axisymmetric case. Asymmetric modes are of major importance as they are numerous compared to axisymmetric ones. Moreover, as non-linear couplings between any modes are possible, an axisymmetric excitation of the structure can lead to asymmetric vibrations (see [1] for example). Experimental investigations on non-linear vibration of shells are very few. Most of them focus on one-mode vibrations and on the associated hardening or softening behavior. Amabili et al. [2,3] experimentally investigated non-linear vibrations of cylindrical shells, coupled with fluid or not, and reported other experimental works. On spherical shells, experimental results on snapthrough behavior are exposed in [4] and a few qualitative experiments on the special case of a 2:1 internal resonance between two axisymmetric modes were reported by Yasuda and Kushida [5]. To the knowledge of the authors, no experiments on multimode asymmetric non-linear response of spherical shells have been proposed yet. A 1:1 internal resonance has been studied in the same manner as here in the case of a circular plate by Thomas et al. [6].

The structure is forced with a harmonic signal of frequency close to the natural frequency ω_3 of an axisymmetric mode (with one nodal circle and no nodal diameters, denoted mode 3). Two companion asymmetric modes (with no nodal circles and 6 nodal diameters, denoted modes 1 and 2) have their natural frequencies ω_1 and ω_2 close to half that of mode 3 ($\omega_3 \approx 2\omega_1 \approx 2\omega_2$). Due to this particular 1:1:2 internal resonance, exchanges of energy between the directly excited mode (mode 3) and the two others are observed. The amplitudes of the three involved modes are measured and compared to the theoretical results presented in [1]. A qualitative validation is obtained, and a quantitative comparison leads to obtain the validity domain of the

* Corresponding author: Tel.: + (33) 1 58 80 85 80; Fax: + (33) 1 47 40 2716; E-mail:oliver.thomas@cnam.fr

theory. Some improvements of the theoretical model are finally suggested.

2. Theoretical model

This section briefly recalls the theoretical results of Thomas et al.[1]. The local dynamic partial differential von Kármán equations are expanded onto the linear mode basis. The dimensionless transverse displacement is then written:

$$w(r,\theta,t) = \sum_{s=1}^{+\infty} \Phi_s(r,\theta) q_s(t) \tag{1}$$

where Φ_s denotes the s-th. mode shape and q_s its time evolution. The latter is solution of:

$$\ddot{q}_s(t) + \omega_s^2 q_s(t) = \varepsilon_q \left[-\sum_{p=1}^{+\infty}\sum_{q=1}^{+\infty} \beta_{pq}^s q_p(t) q_q(t) - 2\mu_s \dot{q}_s(t) + \tilde{Q}_s(t) \right] - \varepsilon_c \sum_{p=1}^{+\infty}\sum_{q=1}^{+\infty}\sum_{r=1}^{+\infty} \Gamma_{pqr}^s q_p(t) q_q(t) q_r(t) \tag{2}$$

where ω_s, μ_s and $\tilde{Q}_s$ are the dimensionless angular frequency, damping coefficient and excitation function of the s-th mode, ϵ_q and ϵ_c are 'small' parameters depending on the geometry of the shell and β_{pq}^s and Γ_{pqr}^s are coefficients that govern the energy exchanges between modes. Their values are related to the mode shapes $\{\Phi_\alpha\}_{\alpha=p,q,r,s}$.

A first order solution $O(\varepsilon_q)$ to the particular 1:1:2 internal resonance is obtained by retaining in (2) the quadratic terms and the three equations related to the three involved modes only. The structure is forced by a harmonic forcing of angular frequency Ω at its center, with $\Omega \approx \omega_3$. The steady-state response is then:

$$w(r,\theta,t) = \Phi_1(r,\theta) q_1(t) + \Phi_2(r,\theta) q_2(t) + \Phi_3(r) q_3(t) \tag{3}$$

$$q_1(t) = a_1 \cos\left(\frac{\Omega}{2} t - \frac{\gamma_1 + \gamma_3}{2}\right), \quad q_2(t) = a_2 \cos\left(\frac{\Omega}{2} t - \frac{\gamma_2 + \gamma_3}{2}\right) \tag{4a}$$

$$q_3(t) = a_3 \cos(\Omega t - \gamma_3) \tag{4b}$$

q_1 and q_2 are related to the asymmetric modes and q_3 to the axisymmetric. The $\{a_s\}_{s=1,2,3}$ and $\{\gamma_s\}_{s=1,2,3}$ are the corresponding amplitudes and phases.

It is shown that three vibratory solutions can be obtained:

- the SDOF solution (single-degree-of-freedom), with $a_1 \equiv a_2 \equiv 0$ and $a_3 \neq 0$, which is the usual uncoupled solution;
- the C_1 solution, with $a_1 \neq 0$, $a_2 \equiv 0$, $a_3 \neq 0$: an energy transfer occurs between mode 3 and 1;
- the C_2 solution, with $a_1 \equiv 0$, $a_2 \neq 0$, $a_3 \neq 0$: an energy transfer occurs between mode 3 and 2.

In the (a_3, Ω)-plane, the SDOF solution is stable outside an instability region, inside which the coupled solutions C_1 and C_2 take birth.

3. Experimental details

The three involved modes and the experimental setup are shown in Fig. 1. The excitation is located at the center of the shell, so that only the axisymmetric mode (mode 3) is directly excited, since the two asymmetric modes have a node at the center. The non-contact exciter already used by Thomas et al. [6] has been chosen here. It is composed of a magnet, glued at the center of the shell, and driven by a coil fed by a sinusoidal electric current.

Three transducers (two accelerometer and a laser vibrometer) are used to measure the time evolutions of the modes. Accelerometer A (resp. B) is located on a node of mode 2 (resp. mode 1) so that it measures the time evolution of mode 1 (resp. mode 2). The laser vibrometer beam points the center of the shell and thus it measures mode 3 time evolution only. The three signals are filtered so that only their fundamental component (of frequency $\Omega/2$ for modes 1 and 2 and of frequency Ω for mode 3) is retained. This operation also eliminates the slight contribution of mode 3 to the accelerometer signals, since points A and B are not located on the nodal circle of mode 3.

The resonance curves of Fig. 2 are measured by holding constant the amplitude of the excitation and measuring the amplitudes of the three filtered transducers signals, for various frequencies of excitations. The measured amplitudes are transformed in displacement amplitudes by assuming that the measured signals are pure sine waves.

The instability region (Fig. 3) is measured by the following procedure: each point of its boundary, related to a particular amplitude of excitation, is obtained by measuring amplitude a_3 and excitation frequency Ω at the precise location where the SDOF solution becomes unstable and coupled solutions arise. This measurement is realized by sweeping forward and backward in frequency, and is repeated for different forcing amplitudes.

4. Results and conclusions

Three resonance curves, obtained with increasing forcing levels, are shown on Fig. 2. For low forcing level, only a SDOF (uncoupled) solution is obtained (case (1),

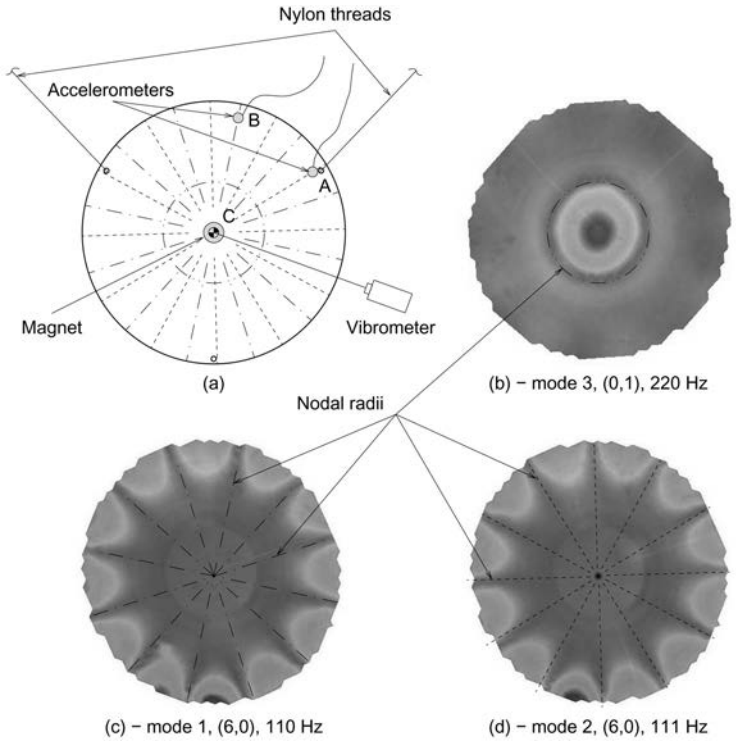

Fig. 1. Experimental setup and mode shapes of the three involved modes.

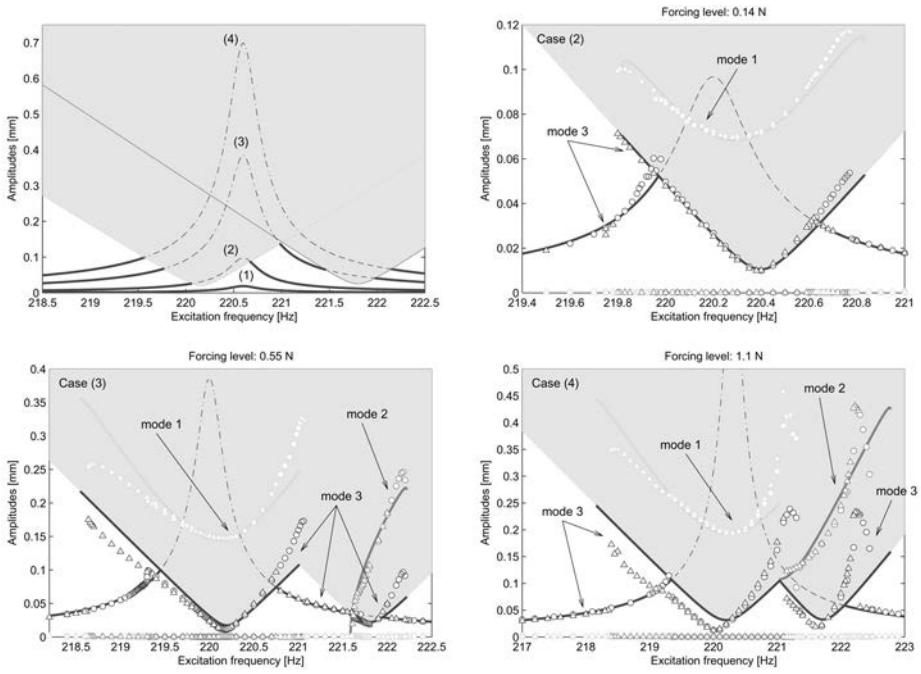

Fig. 2. Amplitudes of the three involved modes as functions of the excitation frequency (('—'): theoretical, ('o', 'Δ'): experimental), for three forcing amplitudes. The gray shaded areas depict the theoretical instability regions and the dash line shows the unstable SDOF solution. Case (1): 0.1 N, SDOF solution only (not shown); case (2): 0.14 N, SDOF and C_1 solutions; case (3), 0.55 N and (4), 1.1 N: SDOF, C_1 and C_2 solutions.

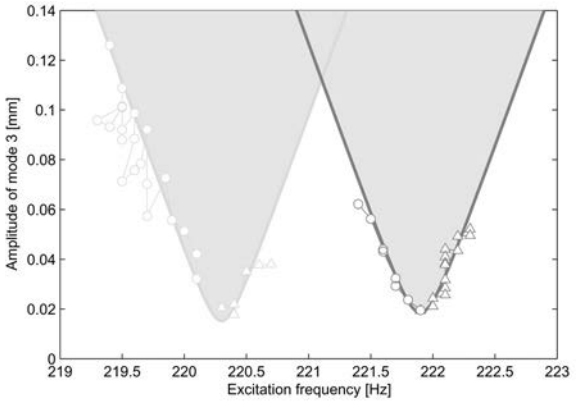

Fig. 3. Instability regions. ('—'): theoretical, ('o','Δ'): experimental.

not shown). Increasing the forcing level, a C_1 (coupling with mode 1) solution appears (case (2)). For a larger forcing, a C_2 solution (coupling with mode 2) is observed, separated from the C_1 solution by a SDOF solution. For an even larger forcing, C_1 and C_2 solutions are followed successively. An excellent qualitative agreement is obtained with the theory, since all those subtle features are predicted by the model.

A quantitative comparison is obtained by adjusting the parameters of the model so that theoretical curves fit the experimental ones. Table 1 gathers the parameters values identified from various experiments. $\{f_i\}_{i=1,2,3}$, $\{\zeta_i\}_{i=1,2,3}$ denote the natural frequencies and damping ratios (equivalent to the dimensionless parameters $\{\omega_i\}_{i=1,2,3}$ and $\{\mu_i\}_{i=1,2,3}$), K is the ratio between the theoretical forcing amplitude and the measured current intensity in the coil, and $\{\alpha_i\}_{i=1,2,3}$ are coefficients of the nonlinear coupling terms, related to β^s_{pq} and Γ^s_{pqr} in (2) (see [1]).

Some discrepancies on the parameters' values are observed, from one experiment to another. Two main conclusions on the validity of the model can be formulated.

- The cubic terms in (2), neglected in the model, should be taken into account. This conclusion is motivated by the fact that some resonance curves of the form of case (1) (i.e. only an uncoupled SDOF solution is obtained) were measured slightly curved toward the low frequencies, a feature characteristic of a cubic non-linearity of the softening type for mode 3. As the correction brought by the cubic terms is of the same order as the non-resonant excitations of the other modes of the system (i.e. $\{q_s\}_{s\neq 1,2,3}$, is small but non zero), the formalism of non-linear modes could be used to keep a 3-degrees-of-freedom model [7].
- Imperfections on the curvature of the shell used in the experiments have been observed. Even if those imperfections are slight, some differences with the theory have been noticed on the location of the nodal circles of the axisymmetric modes. This could explain the discrepancies theory/experiments on the $\{\alpha_i\}_{i=1,2,3}$. The finite element method should be a mean of calculating the $\{\alpha_i\}_{i=1,2,3}$ related to any shell geometry. This will enable to study non-linear oscillations of structure with geometric imperfections and more complex geometries.

References

[1] Thomas O, Touzé C, Chaigne A. Non-linear vibrations of free-edge thin spherical shells: modal interaction rules and

Table 1
Model parameters obtain theoretically by Thomas et al. [1] (first column) and by fitting the theoretical resonance curves to the experimental ones, for various experiments

	Theory (Ref. [1])	Modal anal.	Instab. region (Fig. 3)	exp. (1)	exp. (2) (Fig. 2)	exp. (3) (Fig. 2)	exp. (4) (Fig. 2)
K [N/A]	–	–	–	0.92	0.92	0.92	0.92
f_1 [Hz]	102	110.1	110.13	–	110.2	110.1	110.1
f_2 [Hz]	102	110.86	110.95	–	–	110.9	110.86
f_3 [Hz]	387	220.05	–	220.16	220.2	220	220.3
ζ_1 [%]	–	0.074	0.05	–	0.04	0.06	0.12
ζ_2 [%]	–	0.087	0.06	–	–	0.075	0.10
ζ_3 [%]	–	0.067	–	0.06	0.067	0.067	0.067
α_1	30	–	1.0	–	1.1	1	1.1
α_2	30	–	0.95	–	0.9	1	0.9
α_3	13.8	–	–	–	–	1.3	1.4
α_4	13.8	–	–	–	–	1.3	1.1

1:1:2 internal resonance. International Journal of Solids and Structures 2004, accepted for publication.
[2] Amabili M, Pellegrini M, Tommesani M. Experiments on large-amplitude vibrations of a circular cylindrical panel. J Sound Vib 2003;260(3):537–547.
[3] Amabili M. Theory and experiments for large-amplitude vibrations of empty and fluid-filled circular cylindrical shells with imperfections. J Sound Vib 2003;262(4):921–975.
[4] Evensen HA, Evan-Iwanowsky RM. Dynamic response and stability of shallow spherical shells subject to time-dependant loading. 1967;AIAA Journal 5(5):969–976.
[5] Yasuda K, Kushida G. Nonlinear forced oscillations of a shallow spherical shell. Bull JSME 1984;27(232):2233–2240.
[6] Thomas O, Touzé C, Chaigne A. Asymmetric non-linear forced vibrations of free-edge circular plates, Part II: experiments. J Sound Vib 2003;265(5):1075–1101.
[7] Touzé C, Thomas O, Chaigne A. Hardening/softening behaviour in non-linear oscillations of structural systems using non-linear normal modes. J Sound Vib 2004;273(1–2):77–101.